Available online at www.sciencedirect.com
ScienceDirect
Nuclear Medicine and Biology 37 (2010) 509–516
NUCLEAR MEDICINE AND BIOLOGY
www.elsevier.com/locate/nucmedbio

Carbon-11 labeled papaverine as a PET tracer for imaging PDE10A: radiosynthesis, in vitro and in vivo evaluation

Zhude Tu*, Jinbin Xu, Lynne A. Jones, Shihong Li, Robert H. Mach

Mallinckrodt Institute of Radiology, Washington University School of Medicine, St. Louis, MO 63110, USA

Received 5 December 2008; received in revised form 6 December 2009; accepted 30 December 2009

Abstract

Papaverine, 1-(3,4-dimethoxybenzyl)-6,7-dimethoxyisoquinoline, a specific inhibitor of phosphodiesterase (PDE) 10A with IC_{50} values of 36 nM for PDE10A, 1,300 nM for PDE3A and 320 nM for PDE4D, has served as a useful pharmaceutical tool to study the physiological role of PDE10A. Here, we report the radiosynthesis of [^{11}C]papaverine and the in vitro and in vivo evaluation of [^{11}C]papaverine as a potential positron emission tomography (PET) radiotracer for imaging PDE10A in the central nervous system (CNS). The radiosynthesis of papaverine with ^{11}C was achieved by *O*-methylation of the corresponding des-methyl precursor with [^{11}C]methyl iodide. [^{11}C]papaverine was obtained with ~70% radiochemical yield and a specific activity >10 Ci/μmol. In vitro autoradiography studies of rat and monkey brain sections revealed selective binding of [^{11}C]papaverine to PDE10A enriched regions: the striatum of rat brain and the caudate and putamen of rhesus monkey brain. The biodistribution of [^{11}C]papaverine in rats at 5 min demonstrated an initially higher accumulation in striatum than in other brain regions, however the washout was rapid. MicroPET imaging studies in rhesus macaques similarly displayed initial specific uptake in the striatum with very rapid clearance of [^{11}C]papaverine from brain. Our initial evaluation suggests that despite papaverine's utility for in vitro studies and as a pharmaceutical tool, [^{11}C]papaverine is not an ideal radioligand for clinical imaging of PDE10A in the CNS. Analogs of papaverine having a higher potency for inhibiting PDE10A and improved pharmacokinetic properties will be necessary for imaging this enzyme with PET.

Keywords: PDE10A; PET; Radiotracer; CNS; Phosphodiesterase 10A; C-11; Papaverine

1. Introduction

Phosphodiesterases (PDEs) are a class of intracellular enzymes involved in the hydrolysis of the nucleotides cyclic adenosine monophosphate (cAMP) and cyclic guanosine monophosphates (cGMP) into their respective nucleotide monophosphates. cAMP and cGMP function as intracellular second messengers regulating many intracellular processes particularly in neurons of the central nervous system (CNS). A major mechanism for regulating cyclic nucleotide signaling is by phosphodiesterase-catalyzed cyclic nucleotide catabolism. There are 11 known families of phosphodiesterases encoded by 21 different genes [1–3]. PDE10A is a dual specificity phosphodiesterase that can convert both cAMP to adenosine monophosphate (AMP) and cGMP to guanosine monophosphate; PDE10A is uniquely localized in mammals relative to other PDE families. PDE10A mRNA is reported to be highly expressed in the brain, particularly in striatal medial spinal neurons, with variable expression seen in the testes [1,4]. In human brain, high expression of PDE10A was found in caudate nucleus and putamen of striatum. In other mammalian species PDE10A is enriched in the striatal complex including caudate nucleus, nucleus accumbens and olfactory tubercle [3,5–7]. Outside the brain, PDE10A distribution is limited to a few kinds of tissue, such as the testis, epididymal sperm and enteric ganglia. PDE10A is primarily membrane-bound and it is most often associated with membranes in dendrites and spines of medium spiny neurons, which suggests that PDE10A enables the regulation of intracellular signaling from glutamatergic and dopaminergic input to these neurons [3].

* Corresponding author. Division of Radiological Sciences, Washington University School of Medicine, Campus Box#: 8225, St. Louis, MO 63110, USA. Tel.: +1 314 362 8487; fax: +1 314 362 0039.
E-mail address: tuz@mir.wustl.edu (Z. Tu).

0969-8051/$ – see front matter © 2010 Elsevier Inc. All rights reserved.
doi:10.1016/j.nucmedbio.2009.12.012

Papaverine was identified as a specific inhibitor of PDE10A with an IC_{50} value of 36 nM for PDE10A and IC_{50} values of 1,300 nM for PDE3A and 320 nM for PDE4D [8]. Papaverine proved to be a useful pharmacological tool for investigations of the behavioral effects of PDE10A enzyme inhibition in rodents. Systemic administration of papaverine to genetically modified mice demonstrated inhibition of PDE10A activity and resulted in increased activation of the medial spinal neurons that led to suppression of behavioral responsiveness. The inhibition of PDE10A with papaverine increased the effectiveness of haloperidol-induced catalepsy in rats and inhibited conditioned avoidance responding in mice [8,9]. Papaverine also inhibits the locomotor hyperactivity induced by stimulants [6]. Furthermore, papaverine displayed anti-schizophrenic activity and anti-psychotic activity in different animal models of neurological disorders [8]. As an inhibitor of PDE10A, papaverine not only helped define the physiological role of PDE10A, but it also provided evidence to support the hypothesis that the inhibition of PDE10A mediated cyclic nucleotide hydrolysis might be an effective new approach for the treatment of schizophrenia and other disorders of basal ganglia function.

Positron emission tomography (PET) imaging with appropriate tracers is a highly sensitive non-invasive imaging modality that can measure the densities of neuronal receptors in CNS and thus provide neurological information regarding molecular and cellular function in living subjects. Up to now, no suitable PET tracer for imaging PDE10A enzyme activity has been reported, thus the measurement of PDE10A activity is currently limited to the use of ex vivo immunohistochemistry techniques in tissue. Although radioactive [^{3}H]papaverine [10] and [^{14}C]papaverine [11] have been made for pharmacologic studies, the radiosynthesis of [^{11}C]papaverine and the evaluation of [^{11}C]papaverine as a PET tracer for imaging PDE10A have not yet been reported. Here, we report the radiosynthesis of [^{11}C]papaverine and the initial in vitro and in vivo evaluation of [^{11}C]papaverine as a PET tracer for imaging PDE10A. Papaverine possesses four *O*-methyl groups that can be readily labeled with carbon-11 via *O*-alkylation of the *des*-methyl precursors. We chose 1-(4-(benzyloxy)-3-methoxybenzyl)-6,7-dimethoxyisoquinoline, **4**, as precursor for radiosynthesis of [^{11}C]papaverine, which is based on this position is easy to be metabolized. Metabolic demethylation from this labeling position will result that the metabolite lose the radioactivity carbon-11, which can avoid the formation of radiolabeled metabolites that might cross the blood brain barrier and interrupt measurement of [^{11}C]papaverine in the brain. In this paper, we report the synthesis of precursor **4** and the radiolabeling conditions used to prepare [^{11}C]papaverine via *O*-alkylation of **4** with [^{11}C]methyl iodide. In vitro autoradiographic studies on both rat and macaque brain sections were conducted with [^{11}C]papaverine; the biodistribution and regional brain uptake studies of [^{11}C]papaverine was evaluated in mature male Sprague–Dawley rats. MicroPET brain imaging was carried out using male rhesus macaques. The metabolite studies were performed on rat blood and rat brain post injection of [^{11}C]papaverine. The results of these studies indicated that although [^{11}C]papaverine binds to PDE10A-rich regions of the brain in vitro, the rapid washout of the tracer limits its utility as PET radiopharmaceutical for in vivo measurements of PDE10A.

2. Materials and methods

2.1. Chemistry

2.1.1. General

All analytical grade chemicals and reagents were purchased from Sigma-Aldrich (Milwaukee, WI, USA) and were used without further purification unless otherwise stated. Flash column chromatography was conducted using Scientific Adsorbents, Inc. silica gel, 60a, "40 Micron Flash" (32–63 μm). ^{1}H NMR spectra were recorded at 300 MHz on a Varian Mercury-VX spectrometer. All chemical shift values are reported in ppm (δ).

*2.1.2. 2-(4-(benzyloxy)-3-methoxyphenyl)-N-(2-(3,4-dimethoxyphenyl)-2-hydroxyethyl)-acetamide (**2**)*

A mixture of 2-(4-(benzyloxy)-3-methoxyphenyl)acetic acid, **1** (0.5 g, 1.83 mmol) in 3 ml of thionyl chloride was refluxed for at least 3 h, then the excess thionyl chloride was evaporated under reduced pressure. The residue was dissolved in 8 ml of chloroform, then added dropwise into a pre-cooled mixture of 8 ml chloroform ($CHCl_3$) with 2-amino-1-(3,4-dimethoxylphenyl)ethanol hydrochloride (0.42 g, 1.80 mmol) and 10 ml of 10% NaOH aqueous solution. The reaction mixture was stirred overnight at room temperature. The organic layer was separated out and the aqueous layer was extracted with dichloromethane (3×10 ml). The dichloromethane extraction solutions were combined and washed sequentially with saturated sodium bicarbonate brine and then dried over sodium sulfate (Na_2SO_4). After removal of the solvent by evaporation under reduced pressure, the crude product was purified on a silica gel column with a mobile phase of hexane/ethyl acetate/methanol (50/50/10) to give a brown solid, **2** (0.60 g, 72%). The ^{1}H NMR spectrum (300 MHz, $CDCl_3$) of the purified product was 3.20–3.40 (m, 1H), 3.50–3.52 (s, 2H), 3.52–3.61 (m, 1H), 3.85–3.86 (t, 9H), 4.60–4.80 (s, 1H), 5.14–5.15 (d, 2H), 5.80–6.00 (s, 1H), 6.60–6.90 (m, 6H), 7.20–7.50 (m, 5H), 8.02 (s, 1H).

*2.1.3. 1-(4-(benzyloxy)-3-methoxybenzyl)-6,7-dimethoxyisoquinoline (**3**)*

A mixture of compound **2** (0.5 g, 1.1 mmol) and phosphorous oxychloride ($POCl_3$) (0.34 g, 2.2 mmol) in 30 ml acetonitrile was refluxed for at least 2 h. The solvent was evaporated under reduced pressure. 30 ml chloroform was added into the residue and then additional 10 ml of pre-cooled 50% NaOH aqueous solution was added into the reaction flask. The organic layer was separated, and

the aqueous layer was extracted with dichloromethane (10×20 ml). The combined organic extract was dried over anhydrous Na_2SO_4. After removal of the solvent by rotary evaporation, the crude product was purified on a silica gel column with the mixture of hexane/ethyl acetate/methanol (50/50/5) as mobile phase to give compound **3** (230 mg, 50%). The ^1H NMR spectrum (300 MHz, $CDCl_3$) of the purified product was 3.77 (s, 3H), 3.86 (s, 3H), 4.00 (s, 3H), 4.52 (s, 2H), 5.01 (s, 2H), 6.70–6.83 (m, 3H), 7.05(s, 1H), 7.26–7.43 (m, 6H), 8.35–8.37 (d, 1H).

*2.1.4. 4-((6,7-dimethoxyisoquinolin-1-yl)methyl)-2-methoxyphenol (**4**)*

A mixture of compound **3** (0.23 g, 0.55 mmol) and 4 ml of 10% hydrochloric acid and 2 ml of ethanol was refluxed for at least 2 h until thin layer chromatography (TLC) confirmed that the reaction was complete. The solution was concentrated under reduced pressure. Then 10 ml of 50% NaOH aqueous solution was added into the residue to basify the mixture. The aqueous solution was extracted with chloroform (3×15 ml), and the chloroform extract was dried over anhydrous Na_2SO_4. After concentration under reduced pressure, the crude product was purified on silica gel column with the mixture of hexane/ethyl acetate/ methanol (50/50/5) as mobile phase to give compound **4** (75 mg, 42%) as a pale solid. The ^1H NMR spectrum (300 MHz, $CDCl_3$) of the purified product was 3.75 (s, 3H), 3.90 (s, 3H), 4.00 (s, 3H), 4.52 (s, 2H), 6.77 (s, 1H), 6.82 (s, 2H), 7.05 (s, 1H), 7.30–7.44 (m, 2H), 8.35–8.38 (d, 1H).

2.2. Radiochemistry

2.2.1. Production of [^{11}C]Methyl iodide

[^{11}C]MeI is produced online from [^{11}C]CO_2 using a GE PETtrace MeI Microlab. Up to 1.4 Ci of [^{11}C] CO_2 is produced at the Washington University School of Medicine Cyclotron Facility using a JSW BC-16/8 cyclotron by irradiating a gas target of 0.2% O_2 in N_2 for 15–30 min with a 40 μA beam of 16 MeV protons. The GE PETtrace MeI Microlab converts the [^{11}C]CO_2 to [^{11}C]methane using a nickel catalyst [Shimalite-Ni (reduced), Shimadzu, Japan P. N.221-27719] in the presence of hydrogen gas at 360°C; it is further converted to [^{11}C]MeI by reaction with iodine in the gas phase at 690°C. Approximately 12 min following the end-of-bombardment, several hundred millicuries of [^{11}C] MeI are delivered in the gas phase to the hot cell where the radiosynthesis is accomplished.

2.2.2. Radiochemical Synthesis of [^{11}C]papaverine

The synthesis of [^{11}C]papaverine (Scheme 1) was performed in a gantry system equipped with air-activated valves for remote manipulation of delivery and transfer of solutions. The high-performance liquid chromatography (HPLC) system consisted of a Rheodyne injector valve with 2.0 ml sample loop, a Thermo Separations P200 HPLC binary pump, a Spectra Physics Spectra 100 UV variable detector (250 nm), a Bioscan Flow counter radioactivity

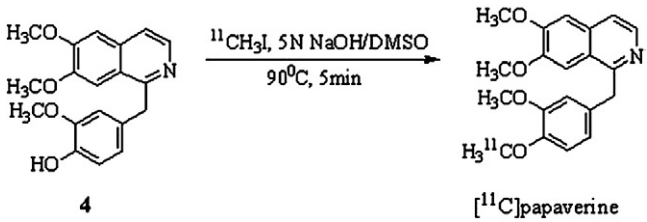

Scheme 1.

detector (NaI crystal), a dual-pen chart recorder and a three-way collection valve. [^{11}C]MeI was bubbled for a period of 3–4 min into a solution of 0.7–1.3 mg of precursor **4** in dimethylsulfoxide (DMSO) (0.18 ml) containing 2 μl of 5 N NaOH at a room temperature. When the transfer of radioactivity was complete, the sealed reaction vessel was heated at 85°C with oil bath for 5 min. The reaction vessel was removed from the oil bath and a solution of the HPLC mobile phase (1.8 ml) was added to the reaction vessel. The residue was injected onto a reversed phase Phenomenex C-18 Prodigy ODS semi-preparative HPLC column (250×10 mm, 10 μA) system to purify the [^{11}C]papaverine. The HPLC mobile phase solution was 25% acetonitrile and 75% 0.1 M ammonium formate buffer (0.1 molar ammonium formate with 1.0 ml of 90% formic acid dissolved into 1 L of milli-Q water, pH value 4.0–4.5) with a flow rate of 3.5 ml/min. Under these conditions, [^{11}C]papaverine was collected from 15.50 to 17.30 min in a 50-ml round bottom flask. The solution was concentrated under reduced pressure. The residue was diluted with saline and filtered through a 0.22-μm pyrogen-free Millipore filter. The saline solution of [^{11}C] papaverine was ready for injection. The total synthesis time was 50–55 min. A 100-μl aliquot of the injectate was sent to the quality control (QC) laboratory for purity and specific activity determination. The QC was run on an analytical HPLC system that consisted of a Phenomenex C-18 Prodigy ODS analytic HPLC column (250×4.6 mm, 5 μA) with UV wavelength as 250 nm. The mobile phase was 40% acetonitrile: 60% 0.1 M ammonium formate buffer at a 1.0 ml/min flow rate. The QC displayed the product was eluted at 4.5 min and was authenticated by co-eluting with nonradioactive standard solution of papaverine. The calculated radiochemical yield was ~70% based on the amount of [^{11}C]MeI at the start of the *O*-alkylation step. The radiochemical purity and the chemical purity were both >99%. The specific activity was >20 Ci/μmol (E.O.B, N=5).

2.3. In vitro autoradiographic studies

Coronal sections (20 μm) were prepared from a snap-frozen Sprague-Dawley rat brain (30 striatal sections on five slides) and a male rhesus monkey brain (six sections through the caudate and putamen) with a Microm cryotome and mounted on Superfrost Plus glass slides (Fisher Scientific, Pittsburgh, PA, USA). Coronal sections were incubated with [^{11}C]papaverine at a concentration of ~9 nM in 50 mM Tris-

HCl buffer with 50 mM NaCl pH 7.4 for 30 min at 25°C. Following incubation, tissue sections were rinsed 5 times at 1 min each time with ice cold buffer containing 10 mM Tris-HCl and 150 mM NaCl at pH 7.4. Digital autoradiography was then performed on all slides using a Packard InstantImager (Packard Instruments) and slides were counted for 40 min. The binding of [^{11}C]papaverine to striatal tissue was visualized clearly in both rat and monkey as shown in representative sections in Fig. 1.

2.4. Biodistribution and regional brain uptake studies

All animal experiments were conducted under IACUC approved protocols in compliance with the Guidelines for the Care and Use of Research Animals established by the Washington University Medical School Animal Studies Committee. Adult male Sprague-Dawley rats (250–300 g) were anesthetized with 2-3% isoflurane/oxygen and [^{11}C] papaverine (approximately 200 μCi/150 μl) was administered via intravenous tail vein injection. Rats were again anesthetized and sacrificed at 5 and 30 min post injection, n=4 rats for each time point. Rat brains were rapidly removed, blotted to remove excess blood and the brain stem, cerebellum, cortex, striatum and hippocampus were separated by gross dissection on a chilled glass plate. The remainder of the brain was also collected in order to determine total brain uptake. Samples of blood, lung, heart, muscle, fat, kidney, liver, and testes were also collected. All samples were counted in a Beckman Gamma 8000 well counter with a standard dilution of the injectate. Tissues were weighed and the percentage of the injected dose per gram of tissue (%ID/g) was calculated. The distribution of [^{11}C]papaverine in brain regions and peripheral tissues is shown in Table 1 and Fig. 2.

2.5. Ex vivo metabolite analysis in rat blood and rat brain

Adult male Sprague-Dawley rats (250–300 g) were anesthetized with 2–3% isoflurane/oxygen and [^{11}C] papaverine (~5 mCi for the 30 min rat and 2.4 mCi for the 5 min rat) was administered via intravenous tail vein injection. Rats were again anesthetized and sacrificed at 5 and 30 min post injection. The whole brain was removed from the rat, and then homogenized on ice with 2 ml of ice-cold acetonitrile after the excess blood was blotted off. Blood samples were collected via cardiac puncture into heparinized syringes. 1 ml aliquots of whole blood were counted in a well counter and then separated by centrifugation at ~15,000 g for 2 min into packed red cells and plasma, which were separated and counted. Alliquots of plasma (400 uL) were deproteinted with 1.2 mL of ice-cold acetonitrile and separated by centrifugation. 200 uL of the supernatants were injected on Phenomenex C-18 Prodigy ODS analytic HPLC column (250×4.6 mm, 5 μA) with UV wavelength as 250 nm. The mobile phase was methanol/0.1 M ammonium formate buffer (40/60, v/v) with 1.2 ml/min flow rate. The HPLC fractions were collected at 1 min intervals for 10 min; the samples were counted in the well counter and counts were decay corrected to the time the first sample of the series was counted. Similarly, a 1 ml aliquot of the brain homogenate was transferred to separate tube, counted in the well counter, then the acetonitrile extract was separated from the tissue pellet by centrifugation and both portions were

Table 1
Biodistribution of [^{11}C]papaverine in 250–300 g male Sprague-Dawley rats (%ID/g)

Tissue	5 min	30 min
Blood	0.246±0.015	0.108±0.020
Lung	0.323±0.048	0.104±0.017
Heart	0.325±0.077	0.092±0.017
Muscle	0.132±0.009	0.071±0.009
Fat	0.124±0.020	0.226±0.026
Kidney	0.743±0.050	0.312±0.054
Liver	3.116±0.256	1.489±0.464
Testes	0.288±0.035	0.094±0.017
Brain	0.154±0.013	0.041±0.007
Brain stem	0.183±0.028	0.043±0.004

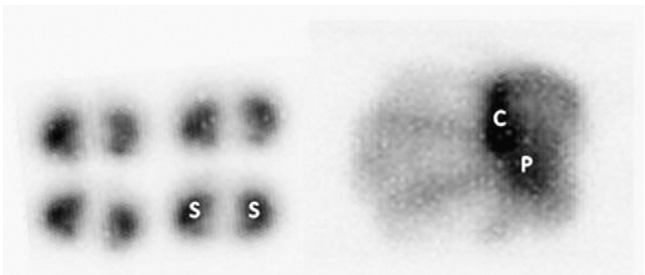

Fig. 1. Autoradiography studies of [^{11}C]papaverine in four representative sections of rat brain (left panel) and one representative section of rhesus brain (right panel) 20 μm sections of rat (30 sections) and monkey (6 sections) brain were incubated with ~5 mCi/ml of [^{11}C]papaverine. Slides were counted for 40 min on the Packard InstantImager. S, striatum; P, putamen; C, caudate.

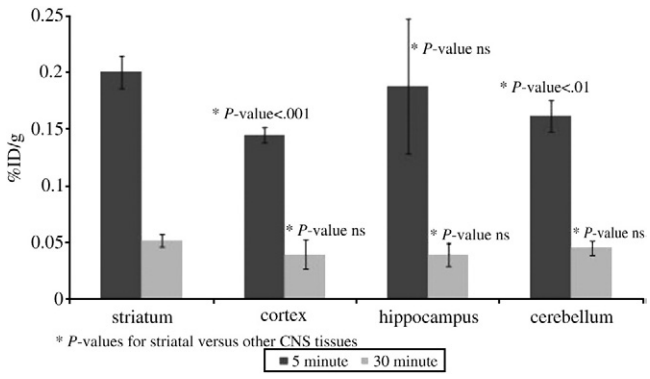

Fig. 2. Regional brain distribution of [^{11}C]papaverine in Sprague-Dawley rats. ~200 μCi/150 μl of [^{11}C]papaverine was injected iv into 250-300g male Sprague-Dawley rats. Rats (n=4) were euthanized 5 and 30 min post injection.

counted. The supernatant was used for radiochromatography as described above, the precipitate was used to calculate for the percent recovery. The percent of unchanged [^{11}C]-papaverine (parent compound) and radiolabeled metabolites were calculated by dividing the amount of recovered radioactivity in the peak by the sum of the total recovered radioactivity in all samples and multiplying by 100. The 30 min brain sample was not processed for metabolite analysis because the total remaining activity was too low (the whole brain at 5 min contained ~2.5 μCi of activity). The results were displayed in Table 2 and Fig. 3.

2.6. microPET studies on rhesus monkey brain

PET studies were performed on two adult male rhesus macaque monkeys (9–9.5 kg) with a microPET Focus 220 scanner (Concorde/CTI/Siemens Microsystems, Knoxville, TN, USA). The animal was fasted for 12 h before PET study. The animal was initially anesthetized using an intramuscular injection with ketamine (10 mg/kg) and glycopyrulate (0.13 mg/kg) and transported to the PET scanner suit. Upon arrival, the animal was anesthetized via an endotracheal tube with 0.75–2.0% isoflurane through the PET scanning procedure. Core temperature was kept constant at 37°C with a heated water blanket. After intubation a percutaneous venous catheter was placed for radiotracer injection. For the microPET scanning session, the head of the monkey was positioned supine in the adjustable head holder, a 10 min transmission scan was performed to check positioning; and once confirmed, a 45 min transmission scan was obtained for attenuation correction. Subsequently, 120 min dynamic emission scanning was acquired coincidently with the administration of ~10 mCi of [^{11}C]papaverine via the venous catheter. Two microPET imaging studies were conducted.

2.6.1. microPET image processing and analysis

Acquired list mode data were histogrammed into a 3D set of sinograms and binned to the following time frames: 3×1, 4×2, 3×3, and 20×5 min. Sinograms were further reconstructed with attenuation correction using the transmission data and scatter correction using direct calculation. The maximum a posteriori (MAP) reconstructions were done with 18 iterations and a beta value of 0.004. A post-reconstruction, smoothing with 1.5 mm Gaussian filter was used for each MAP reconstructed images. By using Amira software (Visage Imaging, Carlsbad, CA, USA), those images were coregistered with magnetic resonance (MRI) images to accurately identify the regions of interest. 3D regions of interest were manually drawn through all planes of coregistered MRI images for the caudate, the putamen and cerebellum. The regions of interest were overlaid on all reconstructed PET images to obtain time–activity curves. Activity measures were standardized to body weight and

Table 2
Metabolite analysis of [^{11}C]papaverine in rat blood and brain

	Peak #1 at 3 min (radioactive metabolites)	Peak #2 at 7 min (parent compound)
5 min brain	4%	96%
5 min blood	26%	74%
30 min blood	78%	22%

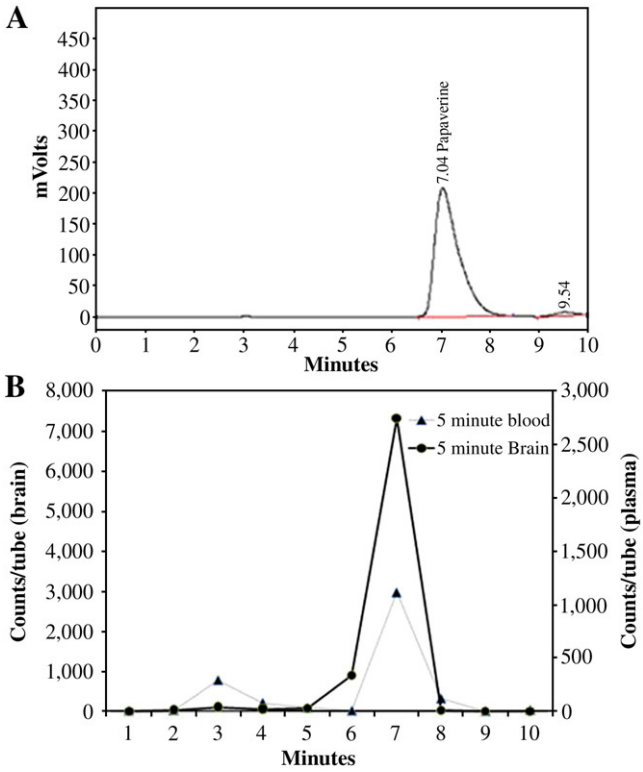

Fig. 3. (A) The chromatography of standard cold papaverine on HPLC with ultraviolet detector, the retention time of papaverine is ~7.0 min. (B) Metabolite analysis of [^{11}C]papaverine in rat plasma sample (dotted line, primary axis) and rat brain (solid line, secondary axis). The second peak at 7.0 min represents the parent compound, [^{11}C]papaverine, the time- radioactivity curve was generated by plotting the counters (after decay corrected) of each 1 min collection sample versus the time.

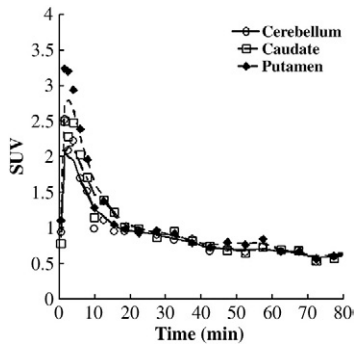

Fig. 4. Time-activity curves of caudate, putamen and cerebellum from a representative microPET imaging study (imaging was performed in two subjects). ~10 mCi of [^{11}C]papaverine was injected into an adult male rhesus monkey (~9 kg) anesthetized with 0.75–2.0% isoflurane. 120 min of dynamic emission scanning was performed.

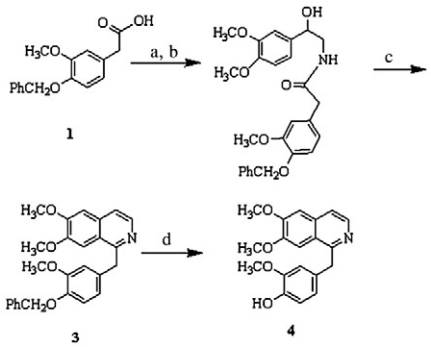

Scheme 2. Reagents: (a) thionyl chloride, reflux; (b) 2-amino-1-(3,4-dimethoxylphenyl)ethanol hydrochloride, 10% NaOH, CHCl3, overnight; (c) POCl3, actonitrile, reflux; (d) 18% HCl, ethanol.

dose of radioactivity injected to yield standard uptake values (SUV) as shown in Fig. 4.

3. Results and discussion

3.1. Chemistry

Papaverine, 1-(3,4-dimethoxybenzyl)-6,7-dimethoxyisoquinoline, possesses four methoxy groups which provide positions that facilitate radiosynthesis of [^{11}C]papaverine using an *O*-desmethylated phenol analogue as precursor reacted with [^{11}C]CH_3I. We choose 4-desmethylpapaverine, **4**, as the precursor for making [^{11}C]papaverine by O-alkylation with [^{11}C]CH_3I using aqueous NaOH solution as base. The synthesis of 4-desmethylpapaverine was accomplished according to Scheme 2 following general methods previously published [12–15]. 2-(4-(Benzyloxy)-3-methoxyphenyl)acetic acid, **1**, was reacted with thionyl chloride to generate 2-(4-(benzyloxy)-3-methoxyphenyl) acetyl chloride. The acetyl chloride was reacted with 2-amino-1-(3,4-dimethoxyphenyl)ethanol hydrochloride to afford 2-(4-(benzyloxy)-3-methoxyphenyl)-*N*-(2-(3,4-dimethoxyphenyl)-2-hydroxyethyl)acetamide, **2**, in 72% yield. The cyclization of **2** by reaction with phosphorus oxychloride generates the 1-(4-(benzyloxy)-3-methoxybenzyl)-6,7-dimethoxyisoquinoline, **3**, in 50% yield. The *O*-debenzylation of **3** by treatment with 18% hydrochloride aqueous solution (HCl) generates the 4-desmethylpapaverine, **4**, in 42% yield. Compound **4** served as the precursor for making the [^{11}C]papaverine.

3.2. Radiochemistry

The radiolabeling of [^{11}C]papaverine was accomplished by employing the convenient conditions for *O*-methylation of phenols with [^{11}C]MeI as shown in Scheme 1. Reaction of the *O*-desmethyl precursor **4** with [^{11}C]MeI in DMSO as solvent and aqueous NaOH as basic catalyst according Scheme 1 gave [^{11}C]papaverine in approximately 70% yield. We found that using DMSO as the reaction solvent with a suitable amount of the NaOH aqueous solution for the reaction O-alkylation step could generate a satisfactory yield of [^{11}C]papaverine. Purification of [^{11}C]papaverine was performed on Phenomenex semipreparative reversed phase C-18 HPLC column. [^{11}C]papaverine was identified by co-eluting with a papaverine standard solution. The retention time of [^{11}C]papaverine on the analytical HPLC system was 4.5 min. The entire synthetic procedure including production of [^{11}C]MeI, HPLC purification and formulation of the radiotracer for in vivo studies, was complete within 50–55 min. [^{11}C]papaverine was obtained in a specific activity >20 Ci/μmol (decay corrected to E.O.B., n=5); the radiochemical and chemical purity were >99%, which is sufficient for in vivo biodistribution and imaging studies.

3.3. In vitro autoradiographic studies

The binding of the [^{11}C]papaverine to PDE10A-rich areas of Sprague-Dawley rat and rhesus macaque monkey brain sections was evaluated by in vitro digital autoradiography using a Packard InstantImager. High [^{11}C]papaverine binding was observed in the striatum of the rat and in the caudate and putamen of rhesus macaque brain sections as shown in Fig. 1. No binding was observed in the surrounding non-striatal tissue of the rat brain. These results are consistent with the regional expression of PDE10A mRNA and protein in the brain because striatal tissue is reported to have a high level of PDE10A enzyme activity in both rats and nonhuman primates [3,5,6].

3.4. Rat biodistribution and regional brain uptake studies

Biodistribution studies were performed using male Sprague-Dawley rats given an intravenous injection of [^{11}C]papaverine. At 5 min post injection, [^{11}C]papaverine displayed heterogeneous distribution in the brain: the striatum had the highest uptake of 0.200%ID/g compared to other brain regions: 0.144%ID/g for cortex; 0.188%ID/g for hippocampus; 0.161%ID/g for cerebellum and 0.154% ID/g for the whole brain (including the striatum) (Fig. 2). This is consistent with reports that the striatum has a high density of PDE10A while the cortex has low PDE10A [1,3,5]. Initial uptake 5 min post injection showed that striatal uptake was significantly higher than cortical uptake (P<.001); 5 min striatal uptake was also modestly higher than uptake in the cerebellum (P<.01). By 30 min post injection, distribution was relatively homogenous: the corresponding uptake of [^{11}C]papaverine was 0.051%ID/g for striatum; 0.039%ID/g for cortex, 0.038%ID/g for hippocampus, 0.045%ID/g for cerebellum, and 0.041%ID/g for total brain. Nonspecific retention of [^{11}C]papaverine in the total brain and specific binding in the striatum was relatively low at 30 min; no significant difference remained in the regional brain distribution of radioactivity. At 30 min post injection, retention of [^{11}C]papaverine in the striatum was only 20 ~30% of that seen at 5 min post injection while blood levels dropped from 0.246%ID/g at 5 min to

0.108%ID/g at 30 min, which means it washed out of the rat brain. The blood clearance is consistent with reports that papaverine is rapidly metabolized in rat plasma with only a 15 min biological half-life in rat plasma [16]. Pharmacological studies also reported that the activation of papaverine on cAMP and phosphoproteins declines after 15 min [8]. Peripheral clearance organs, i.e., the liver and kidney, had higher retention of [^{11}C]papaverine than the CNS. The 30 min kidney activity level was 0.312%ID/g which is 42% of the 5 min value. Even at 30 min post injection, the uptake of [^{11}C]papaverine remained 1.489% ID/g for liver which was 48% of the 5 min uptake (Table 1). The liver uptake of 3.112%ID/g at 5 min post injection represented approximately 32% of the total dose injected into the rat (calculations not shown).

3.5. Ex vivo metabolite analysis in rat blood and rat brain

The plasma radioactivity 5 min post injection displayed 74% parent compound with a retention time of 7.0 min, this peak was confirmed to be the parent compound by injection of cold papaverine into the HPLC system (Fig. 3A and B) that used for metabolite analysis. In addition, 26% of the observed plasma radioactivity was metabolites with a retention time of around 3 min. In comparison with the 5 min blood sample, for the 5 min brain sample, 96% of the observed radioactivity was parent compound while <4% radioactive metabolites were observed as shown in Table 2 and Fig. 3B. The HPLC results also indicated that the metabolites are hydrophobic compared to [^{11}C]papaverine. For the 30 min blood sample, plasma radioactivity at 30 min post injection indicated that only 22% parent compound remained while 78% of the activity was observed to be the radiolabeled metabolites (Table 2). There was insufficient activity remaining in the brain 30 min post injection for HPLC analysis. The structural identification of metabolites was not performed. We like to point out that the mobile phase used for metabolite analysis and flow rate is different from the quality control HPLC system used for reporting the quality of final dose quickly before injected into the animal for pharmaceutical studies. In addition, our quality control laboratory of radiopharmaceuticals limits each carbon-11 sample running time in order to handle quality controls for multiple radiopharmaceuticals in restricted time. In our metabolite analysis HPLC system, we choose methanol/0.1 M formate buffer mobile phase, flow rate at 1.2 ml/min, the retention time of papaverine is 7.0 min (Fig. 3).

The high hydrophobicity of the observed metabolites, and the overwhelming predominance of parent compound in the rat brain at 5 min post injection, suggest that the radiolabeled metabolites observed in the rat blood were unable to cross the blood-brain-barrier and enter into the brain. Based on these observations, during the early time (from 0-5 min) post injection, accumulation of radioactivity in the rat brain may represent [^{11}C]papaverine rather than radiolabeled metabolites.

3.6. microPET scan of a rhesus macaque with [^{11}C]papaverine

Brain microPET imaging was performed on two 9–9.5 kg rhesus macaque monkeys. Studies were performed on two separate days. After intravenous injection of ~10 mCi [^{11}C]papaverine, radioactivity in brain quickly peaked at ~3 min post injection with SUVs of ~3.2 in putamen, ~2.5 in caudate and 2.2 in cerebellum with no significant accumulation in other brain regions. The initial uptake of [^{11}C]papaverine in the caudate and putamen is consistent with literature reports [3,5,6] that PDE10A is only located in striatal tissues of the brain. By 10 min post injection of [^{11}C]papaverine, regional brain distribution was rather homogeneous and no conspicuous accumulation of the radioactivity remained in the caudate or putamen by visual inspection of the PET image (data not shown). As displayed by the time activity curves, although initial uptake of the tracer in the brain was acceptable, by 10 min post injection, the radioactivity rapidly washed out for all brain regions as shown in Fig. 4. These observations are consistent with rapid in vivo clearance of [^{11}C]papaverine from PDE-10 enriched areas of the CNS in rats. Our imaging data may indicate that the 30-nM binding affinity of papaverine, when coupled with a reduced input function due to rapid clearance of papaverine from the blood result in CNS binding kinetics which are unsuitable for a radiotracer [10,17]. Although clinical PET imaging studies with Carbon-11 tracers seldom require prolonged retention in target-areas, the radioactivity uptake ratios of [^{11}C]papaverine in both caudate and putamen to cerebellum at the time of transient equilibrium (10 min post injection) was close to unity, as can be inferred from the data shown in Fig. 3. Although it is necessary to perform the arterial blood metabolism studies for a promising PET radiotracer prior to evaluation in human being, the arterial blood metabolism studies of [^{11}C] papaverine in non-human primate were not performed because of the rapid metabolism of [^{11}C]papaverine in rats and the unencouraging initial imaging results of [^{11}C] papaverine in monkeys.

4. Conclusions

We have successfully prepared [^{11}C]papaverine which has high affinity for PDE10A and moderate selectivity of PDE10A versus PDE3A. This C-11 labeled radiotracer binds in vitro predominantly to PDE10A enriched areas of rat and monkey brain. In vivo evaluation with biodistribution and regional brain uptake studies in rats and microPET brain imaging studies in rhesus macaques demonstrated that [^{11}C] papaverine was able to enter the brain and initially accumulated in PDE-rich regions of the brain. However, after reasonable initial brain uptake, the rapid clearance of [^{11}C]papaverine from the CNS resulted in low retention of radioactivity in striatum by 10 min post injection. Our initial

evaluation showed that [^{11}C]papaverine will not be able to serve as a useful PET radiotracer for clinical imaging of PDE10A in the CNS. Exploring papaverine analogs to identify compounds with higher (subnanomolar) potency and selectivity for PDE10A and suitable pharmaceutical properties is necessary to identify a PET tracer for noninvasive clinical imaging of PDE10A in vivo.

Acknowledgments

This research was supported by the National Institutes of Health grants: DA 16181 and NS48056.We would like to thank Dr. Joel S. Perlmutter and his staff for their assistance with the nonhuman primate microPET imaging process.

References

[1] Fujishige K, Kotera J, Michibata H, Yuasa K, Takebayashi S, Okumura K, et al. Cloning and characterization of a novel human phosphodiesterase that hydrolyzes both cAMP and cGMP (PDE10A). J Biol Chem 1999;274:18438–45.

[2] Kehler J, Ritzen A, Greve DR. The potential therapeutic use of phosphodiesterase 10 inhibitors. Expert Opin Ther Pat 2007;17: 147–58.

[3] Xie Z, Adamowicz WO, Eldred WD, Jakowski AB, Kleiman RJ, Morton DG, et al. Cellular and subcellular localization of PDE10A, a striatum-enriched phosphodiesterase. Neuroscience 2006;139: 597–607.

[4] Fujishige K, Kotera J, Omori K. Striatum- and testis-specific phosphodiesterase PDE10A isolation and characterization of a rat PDE10A. Eur J Biochem 1999;266:1118–27.

[5] Coskran TM, Morton D, Menniti FS, Adamowicz WO, Kleiman RJ, Ryan AM, et al. Immunohistochemical localization of phosphodiesterase 10A in multiple mammalian species. J Histochem Cytochem 2006;54:1205–13.

[6] Seeger TF, Bartlett B, Coskran TM, Culp JS, James LC, Krull DL, et al. Immunohistochemical localization of PDE10A in the rat brain. Brain Res 2003;985:113–26.

[7] Soderling SH, Bayuga SJ, Beavo JA. Isolation and characterization of a dual-substrate phosphodiesterase gene family: PDE10A. Proc Natl Acad Sci U S A 1999;96:7071–6.

[8] Siuciak JA, Chapin DS, Harms JF, Lebel LA, McCarthy SA, Chambers L, et al. Inhibition of the striatum-enriched phosphodiesterase PDE10A: a novel approach to the treatment of psychosis. Neuropharmacology 2006;51:386–96.

[9] Siuciak JA, McCarthy SA, Chapin DS, Fujiwara RA, James LC, Williams RD, et al. Genetic deletion of the striatum-enriched phosphodiesterase PDE10A: evidence for altered striatal function. Neuropharmacology 2006;51:374–85.

[10] Belpaire FM, Bogaert MG. The excretion of 3H-papaverine in the rat. Biochem Pharmacol 1973;22:59–66.

[11] Ithakissios SD, Tsatsas G, Nikokavouras J, Tsolis A. Synthesis of papaverine and quinopavine specifically labeled with ^{14}C. J Label Compounds 1974;10(3):369–79.

[12] Brochmann-Hanssen E, Hirai K. Opium alkaloids. VII. Isolation of a new benzylisoquinoline alkaloid. Synthesis and NMR studies of papaveroline trimethyl ethers. J Pharm Sci 1968;57:940–3.

[13] Brossi A, Teitel S. Selective *O*-demethylation of papaverine. J Org Chem 1970;35:1684–7.

[14] Walker KA, Boots MR, Stubbins JF, Rogers ME, Davis CW. 1-(4-Aminobenzyl)-and 1-(4-aminophenyl)isoquinoline derivatives: synthesis and evaluation as potential irreversible cyclic nucleotide phosphodiesterase inhibitors. J Med Chem 1983;26:174–81.

[15] Rae ID, Simmonds PM. The structure of papaverine in solution as determined by proton nuclear magnetic relaxation methods. Aust J Chem 1987;40(5):915–23.

[16] Belpaire FM, Bogaert MG. Metabolism of papaverine. II. Species differences. Xenobiotica 1975;5:421–9.

[17] Belpaire FM, Rosseel MT, Bogaert MG. Metabolism of papaverine IV. Urinary elimination of papaverine metabolites in man. Xenobiotica 1978;8:297–300.